



# Magnetic pulse welding—investigation on the welding of high-strength aluminum alloys and steels as well as the influence of fluctuations in the production on the welding results for thin metal sheets

Anatoli Rebensdorf<sup>1</sup> · Stefan Böhm<sup>1</sup>

Received: 15 November 2016 / Accepted: 10 January 2018 / Published online: 8 May 2018  
© International Institute of Welding 2018

## Abstract

As there has been an increasing demand for cold welding methods recently, this offers the chance and possibility to use the potential of magnetic pulse technology to its full extent. This is especially the case when joining different materials (steel–aluminum sheet metal welds) and having to adhere to the specific requirements of lightweight constructions, thus, giving this welding method a particular role. In this paper and the oral presentation, results of a publicly funded project will be presented (AiF-Nr. 18290 N/P1029). The focus lies on the weldability of mixed-material combinations through magnetic pulse technology and its reproducibility. Tests showed that, aside from the influence of the surface properties, it is the mechanical properties and chemical composition of the materials that are especially important for the process stability. The generated process window illustrates the aforementioned, whereby the lower curve—surface preparation—can be adapted to meet fluctuations and tolerances in the production. On a secondary level, the robustness of the process is shown as regards fluctuations and tolerances of the process. The results show relevant differences, especially for the alignment of the welding partners as even a change in the discharge energy influences the weld results. The influence of deviations from the angle for a parallel alignment of the metal sheets, the influence of fluctuations in the gap, and the increase in discharge energy are determined and characterized through destructive tests with fragmentation pattern analyses. In sum, the results show the high potential of magnetic pulse welding for the joining of mixed materials and show a high reproducibility of the welding results.

**Keywords** Reproducibility · Fluctuations in production · Mixed-material combinations

## 1 Introduction

The trend to be energy efficient has had an effect on industrial designs such as the concept to use multi-material constructions. Here, the aim is to combine the technical properties of the materials in such a way that these properties can be used

optimally and that the constructions are as light as possible [1]. As the proper joining technique allows to create material compounds which fulfill both the technical requirements and the necessity to reduce weight within the constructions, much research has been focused on the search for adequate techniques to join these materials in order to construct multi-material designs.

In this context, aluminum–steel compounds are especially interesting [1], as they are the materials mostly applied in the industrial areas of mechanical engineering, vehicle constructions, and structural engineering. So far, the applied joining techniques have specific disadvantages, making further research on the suitable joining techniques for this material combination all the more necessary.

The most common joining method for Al–St joints is currently mechanically joining [1]. However, this has the disadvantage of being limited to certain materials and that the strength of the joint depends strongly on the direction of the

---

Recommended for publication by Select Committee AUTO - Automotive and Road Transport

---

✉ Anatoli Rebensdorf  
a.rebensdorf@uni-kassel.de

Stefan Böhm  
s.boehm@uni-kassel.de

<sup>1</sup> Department for Cutting and Joining Manufacturing Processes, University of Kassel, Kassel, Germany

load. A further “cold” joining method for mixed materials is adhesive bonding. But here, the adherends need to be pre-treated with care and this method needs an additional apparatus which holds the pieces in place while the adhesives cure. Furthermore, this joining method is not very resistant to aging processes.

Apart from using cold joining processes, thermal joining processes are also applied to join mixed materials. Here, braze welding processes [2, 3] need to be distinguished from friction welding processes [4]. Braze welding needs a clean process execution to achieve the smallest possible intermetallic phase and, thus, to avoid a brittle fracture of the weld. Additionally, this method induces much heat into the constructional elements. Friction welding, on the other hand, often needs elaborate clamping devices to absorb the reaction forces and the period of the welding process is not efficient enough to be used without limits. For these reasons, the search for new joining methods for steel and aluminum is still highly relevant.

Here, magnetic pulse technology, a method which has been known for quite some time, has become increasingly interesting for researchers and producers alike. This method can easily weld aluminum to steel. Furthermore, the intermetallic phase is extremely thin and can be avoided completely, thus, principally preventing a brittle fracture in the welding zone. This welding method would allow the integration of steel materials into lightweight constructions, e.g., crash boxes in automotive constructions. In addition, magnetic pulse welding produces large weld seam lengths with few cycle periods, which makes this method highly productive.

## 2 Motivation

Scientific publications [5–9] have described previously realized aluminum–steel welds via magnetic pulse technology. Here, a striking fact is that steels with low strength and high formability were mainly chosen for the tests. The choice of aluminum was more varied; in some cases, soft, nearly pure aluminum alloys was used, and in other cases, they were naturally hard and heat-treatable. However, no paper dealt with the reproducibility of the results; the only concession was the comparison of the achievable tensile shear strengths, which was used to interpret the reproducibility of the process.

However, although the phenomenological aspects of the joints were described explicitly (e.g., wave formation), hardly any publication correlated the strengths to these phenomenological examinations. The publication by [10] is an exception; here, the thickness of the intermetallic phase was correlated to the tensile shear strength. Possible improvements of the weld, such as activating the weld formation by modifying the surface of the welding partners, were generally not considered. Surface modifications can shift the stable process window to

low electric currents, increasing the lifespan of the coils and making it possible to join alloys which are difficult to weld.

The limits for the process of magnetic pulse welding of metal sheets are set by the thickness of the sheets, the strength of the flyer material, and its conductivity. However, theoretically, there should be no boundaries for this process, but the following mechanical properties limit the application: the maximum load of the capacitor, the maximum charge for the electric elements, and the maximum charge of the coil. Currently, this limits the sheet thickness to a maximum of 2 mm. The length of the weld seams (which can be produced with one “shot”) can be several meters. Depending on the strength and the electric conductivity of the flyer material, the weldable sheet thickness can decrease significantly.

So far, there are no clear results regarding the achievable manufacturing tolerances. As there is very little heat impact during the process, which is characterized by the very thin and avoidable intermetallic phases, there are only slight deformations. Therefore, the welds will most likely be of high quality and size accuracy [11, 12].

In sum, we aim to describe the specific properties of the weld and to examine the disturbance variables and their influence on the weld, the latter hardly having been examined in research so far.

## 3 Experimental

### 3.1 State of the art and bond formation under impact welding

The method magnetic pulse technology allows to perform the following manufacturing processes: reshaping, shaping, cutting, pressing, and welding. Furthermore, this method is classified as a high-speed process with a characteristic rate of deformation of more than  $10^4 \text{ s}^{-1}$  [13]. In this process, the elements are accelerated to velocities which reach the supersonic range of air. Due to these properties, this method is related to explosion welding (EXW) which reaches similar ranges of deformation.

The technological installation consists mainly of two major components. One is the charging circuit in which a capacitor bank is charged with several kilojoules of charging energy. Secondly, the system has an electric resonant circuit to which the capacitor is connected via high-current switch. The tool for magnetic pulse technology, namely the coil, is set within the electric resonant circuit. This coil impinges the impact energy on the material work piece which is to be formed [14]. Current developments, especially regarding the lifespan of the components, helped to develop this method further so that it is now suited for serial industrial productions.

The impact energy of this method is the magnetic pressure which is created by opposed magnetic fields and is defined by

the discharge energy of the capacitor, the coil, and the material work piece. The primary magnetic field is created through the impulse-like discharge of the capacitor through the coil. The short time span of the discharge, 25–100  $\mu\text{s}$ , forms a magnetic field which varies strongly [15]. Within the work piece, a secondary magnetic field is caused by the physical effects as described by Faraday, Lenz, and Lorentz and is opposed to the primary field which drives the work piece away from the coil (Fig. 1).

Current research on magnetic pulse welding of aluminum and steel is mainly performed within the area of forming technology. The papers [5, 7–10, 16–19] describe studies on aluminum–steel welds. However, the focus lies on the phenomenological description of the welding results.

The strength of various mixed-material welds has often been examined. Generally, the weld seam is regarded to be good if it tears within the base material in tensile shear tests [5]. [7] presents the highest number of samples which were welded with the same parameters, ten samples with the same parameters in every testing series. The base material failed in 80% of the cases; in 20% of the cases, however, the weld seam failed. However, the process was still described as suitable in [5], an opinion which was taken up in [10] although the explanation for the coincidental failure of some components under the same process parameters and surrounding conditions was not given.

Furthermore, the database in [7] is rather small. Welding tests were performed and the location of the fracture of the weld seam and the according forces were documented. In this case, the weld seam also appeared stronger than the base material, but a statement regarding the reproducibility could not be made.

### 3.2 Materials and system technology

Only aluminum–steel welds were examined in the publicly funded research project “PulsRepeat” (AiF-Nr. 18290 N/P1029). The main focus was to describe the weld

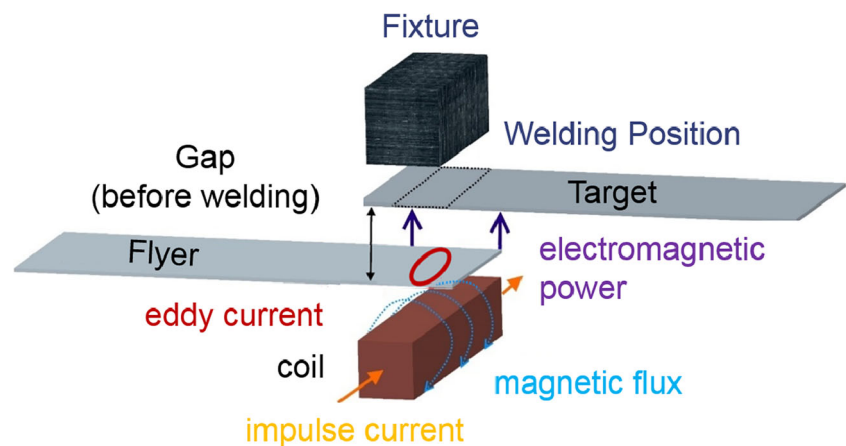
characteristics and to examine the reproducibility in different load scenarios and requirements. For the description of the characteristics of the weld, the strength values, fracture patterns, and metallographic analyses were taken into account. The setup for the preparation of the testing sample is shown in Fig. 2:

In addition, Fig. 2 shows the conditions of collision for magnetic pulse welding. These can be described with the help of the example of an asymmetrical impact welding process in explosion welding (EXW). During impact, the flyer hits the target with a dynamically changing collision angle  $\beta$  at a point of collision/stagnation  $S$ . Here, the collision point velocity  $V_{c,p}$  according to Crossland in [20] is caused by the geometrical relation between the sheet velocity  $V_p$  and the collision angle.

According to the state of the art, the physical process parameters are decisive for the weld formation, especially the jet, also called the mass flow, which is created through the high pressure and is formed from the weaker material. Among other functions, the jet cleans the surface and activates the joining process. This makes it especially necessary to examine the effect of the surface topography, an issue which has been addressed in several studies [21–23]. However, the influence of modifications of the surface, especially on welds combining high-strength materials, has never been examined. Thus, this project used surface modifications not only to activate the surface but also to increase the weld formation when the collision angles are smaller [23]. In addition, the following questions were addressed:

- Can the reproducibility for the magnetic pulse welding of aluminum–steel welds be guaranteed?
- Can the process window be changed when taking into consideration the surface topography?
- Which disturbance variables influence the weld and how can they be bridged while taking into account the process parameters?
- How do magnetic pulse welds react in corrosion and climate change test?

**Fig. 1** Schematic depiction of magnetic pulse welding



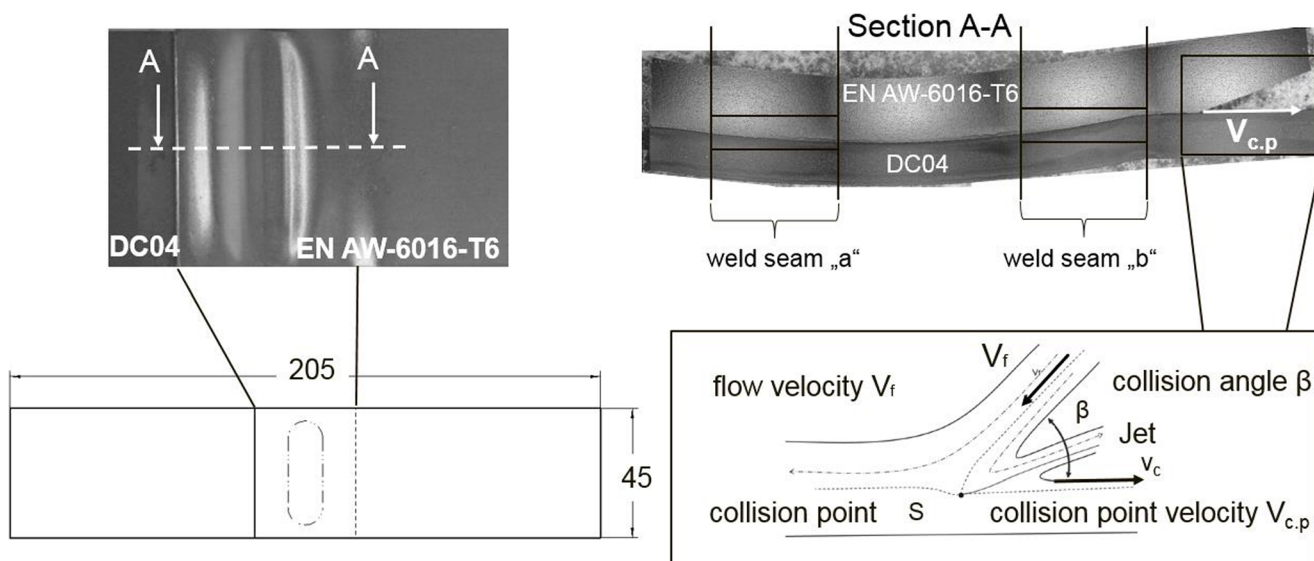


**Fig. 2** Procedure of metallographic analysis and conditions of collision for impact welding

- Can mixed material welds of high-strength and ultra-high-strength materials be achieved?

To answer these questions, the geometry of the testing samples was set to  $(120 \times 45)$  mm. The quasi-static test of the weld properties was performed following the standard DIN EN ISO 14273. An additional peel test following the standard DIN EN ISO 14270 was also performed. The samples were welded in an untreated condition (cleaned with ethanol) and in a treated condition (surface pre-treatment). In the latter case, we also distinguished between laser ablation and polishing. We used the laser system CleanLaser CL50 for the laser ablation. The pulse frequency was 200 kHz, and the distance to the sample was 340 mm. The utilization level was set to 50% with an infeed rate of 8.500 mm/s.

The welding system BlueWave PS 48-16 was used for welding. With a discharge energy of about 20 kJ, the system

technology allowed a transfer of a maximum electric impulse of up to 480 kA to the coil. The maximum discharge energy of the capacitors was 48 kJ with voltages of up to 16 kV. The flat coil B80/5 was used for testing. Table 1 offers an overview of the material combinations which were tested.

## 4 Results

### 4.1 Influence of the surface topography on the reproducibility of the weld

The main tests were performed on welds with the material combination: EN AW-6016-T6 as well as DC04. The influence of the surface topography was examined in relation to the process parameters. The acceleration distance ( $h$ ) and the discharge energy ( $E$ ) were varied. This inevitably influenced the

**Table 1** Overview of the material properties

Materials	Thickness (mm)	Tensile shear strength (MPa)	Yield strength (MPa)
EN AW-Al Mg3 (EN AW-5754-H22)	1	246	189
EN AW-Al Si1.2Mg0.4 (EN AW-6016-T6)	1.25	211	107
DC04	1	289	159
HX420LAD + Z100MB	1.2	545	470
DP600	2	600–700	330–410
DP780 + GI	2	780–900	500–600
22MnB5 + AS 150 (not hardened)	1.5	500–700	350–550
22MnB5 + AS 150 (press hardened)	1.5	1.300–1.650	1.000–1.250

collision angle [23] which grew with increasing acceleration distance. The discharge energy and the linked maximum impulse current ( $I$ ) influence the impact velocities and the collision point velocities. All in all, the amount of the testing samples ( $n$ ) was 8 samples for each testing series. The results are shown in Fig. 3.

The testing series 63.X achieved the best results. Here, the welding distance was 1.5 mm and the discharge energy was set to 17 kJ ( $I = 370$  kA). Both components were pre-treated with laser ablation prior to welding. Under quasi-static tensile stress, this hybrid weld achieved strengths of up to 177 MPa ( $R_m$  of EN AW-6016-T6 was 211 MPa). Testing for normal distribution according to the Anderson-Darling test (0.544) confirmed the significance of the results. The median of this testing series was 175 MPa. The standard deviation was 1.55 MPa, thus, on a small level. A striking fact was that a surface pre-treatment was not necessary. The testing series with the parameters  $E = 17$  kJ ( $I = 370$  kA) and  $h = 1.25$  mm showed similar results, although in this case, no surface pre-treatment was performed. Here too, there was, compared to the other untreated series which seemed to be realized at the lower limit of the process window, hardly any dispersion of the strength values. However, there is a clear tendency that laser ablations had some influence, especially on reproducibility. The laser ablation of steel was enough to achieve good results with low currents ( $I > 300$  kA) and, thus, influenced the stability of the process window in a positive way.

### 4.2 Influence of variation of production and tolerances

In order to be suited for industrial applications, important issues regarding stability of this method need to be addressed.

Here, the examination of the influence of variations in production as well as tolerances aims to make a contribution. In this case, the material combination of an aluminum wrought alloy EN AW-6016-T6 and DC04 was mainly tested. The dimensions of the testing samples were the same in all tests and were in accordance to DIN EN ISO 14273.

The following product-related aspects were examined:

- *Influence of variations of the gap and specific changes of the current or the discharge energy:* The acceleration distance was varied from 1.0 to 2.0 mm in steps of 0.5 mm. The set discharge energy was  $E = 13$  kJ,  $E = 15$  kJ as well as  $E = 17$  kJ.

When looking at the procedural parameters, there is a clear relation between the acceleration distance and the current. Welding with a current of  $I = 370$  kA achieved the highest results for all acceleration distances and the dispersion was very low. If the current is lowered to under 350 kA, the acceleration distance of 1.5 mm showed the best results (Fig. 4).

The testing samples all broke in the weld seams. However, relative strengths of the welds of 0.89 could be achieved. The analysis of the fracture pattern in Fig. 5 exemplarily shows the weld as formed by magnetic pulse welding. At first sight, the elliptic weld seam appears to have a homogenous connection. For better analysis, the steel sample was exposed to color etching according to Weck. The weld seam was separated into three areas, the middle area (no connection), both weld seams, and the pressurized deformation zone of the weld when leaving the process window with an increasing collision angle. Figure 5 shows these areas after tensile shear testing. The welding parameters were  $h = 1.5$  mm as well as  $I = 350$  kA. The relative strength of the weld was 0.79.

Fig. 3 Influence of the surface topography on the material combination EN AW-6016-T6 and DC04

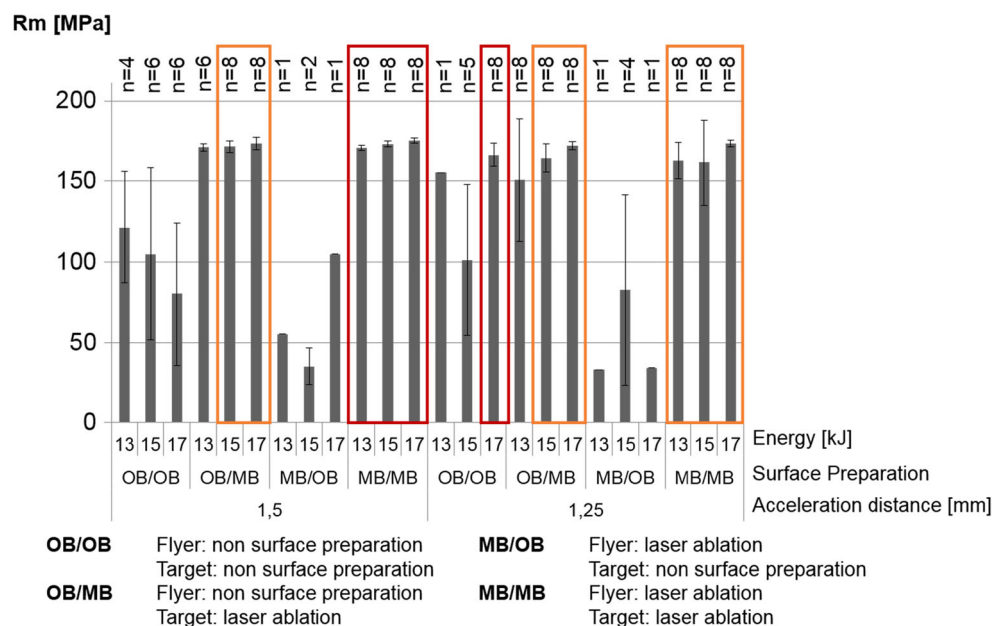


**Fig. 4** Influence of variations of the gap and specific changes of the electrical current

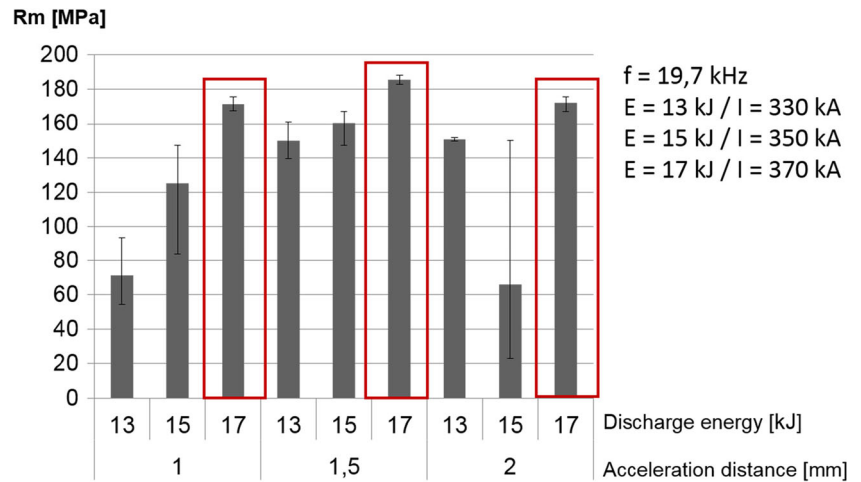


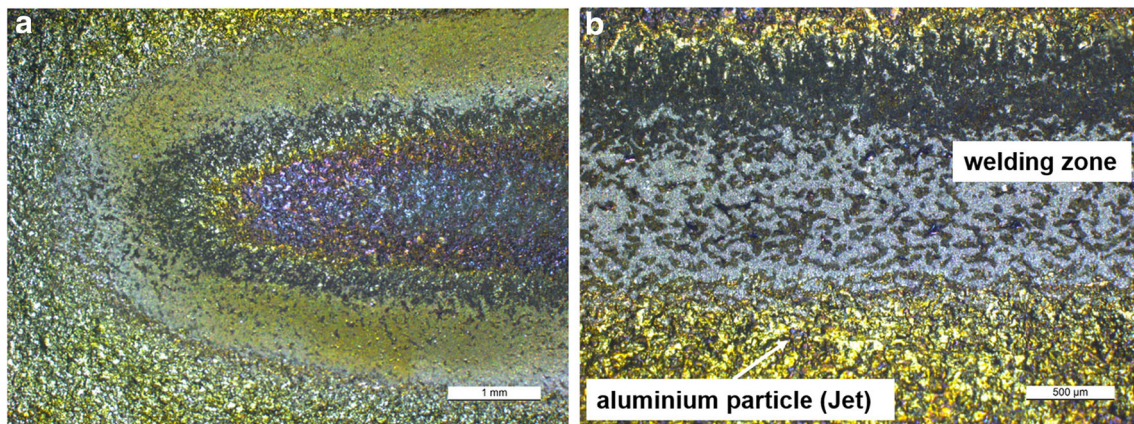
Figure 6 shows the fracture pattern after peel testing. Here, the welding parameters were  $h = 1.0 \text{ mm}$  and  $I = 370 \text{ kA}$ . The fracture pattern clearly shows the aluminum remains in the DC04. This exemplifies the achieved strength values. Once the acceleration distance was decreased (smaller collision angle with high collision point velocities) the intensity of the weld, i.e., the density of the weld seam, increased.

The testing series V8.X with the short acceleration distance achieved higher elongation at break values and higher tensions, respectively transfer of higher tensions. Figure 7 shows the averaged courses of the individual testing series (compare Fig. 4 and the welding parameters).

It is important to note that the choice of the welding parameters influences the properties of the weld. There are direction-dependent weld seam properties which have to be taken into consideration regarding the different testing stresses. As soon as a peeling test is used, the quality of the weld depends on the electrical current. According to the tests in [23], there is a higher collision point velocity in these cases which achieves a higher energy input per time unit and induces the plastic deformation and, thus, the weld formation. For peel testing,

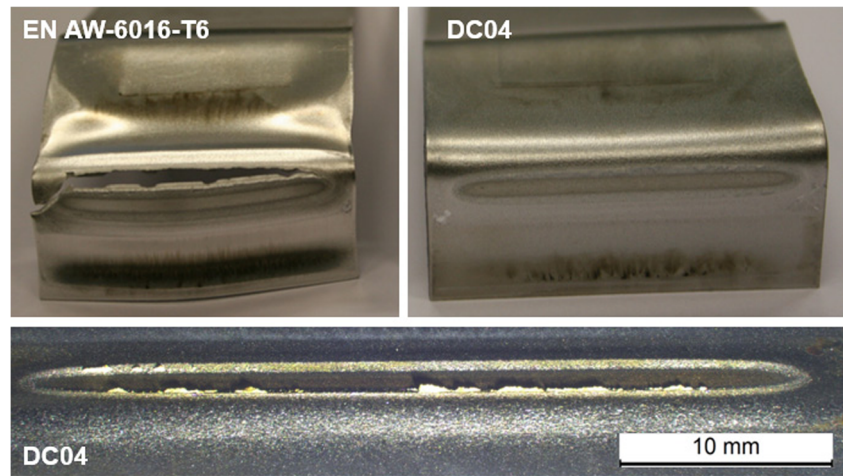
the collision angle should be decreased to achieve shorter acceleration distances in order to increase the density of the weld. The microsections (Fig. 8) confirm these conclusions. This testing series offers no indications for intermetallic phases.

Figure 8a shows a weld, formed with the parameters  $h = 1.0 \text{ mm}$  and  $I = 350 \text{ kA}$ . The weld seam has a straight interface. Wave formation, as suggested in scientific publications, did not occur in this testing series. However, if the current is increased to  $I = 370 \text{ kA}$  while having the same acceleration distance (Fig. 8b, c), an increasingly wavy interface can be observed. Here, the amplitudes stayed below  $20 \mu\text{m}$ . Furthermore, there is an increase in collision point velocity for the steel alloy, encasing fragments in the aluminum (Fig. 8c). In this case, the advantages of the cold joining method magnetic pulse welding, as described at the beginning, show clearly. The physical–chemical properties of the weld formation do not show the typical weld seam irregularities of conventional welding methods (e.g., crack formations, intermetallic phases), a fact which shows the suitability for mixed-material combinations.



**Fig. 5** Analysis of the fracture pattern of DC04 after quasi-static tensile shear testing according to DIN EN ISO 14273

**Fig. 6** Fracture pattern after peel testing according to DIN EN ISO 14270



- *Differences in the orientation of the welding partners have an influence on samples where the overlapping lengths were varied:* The overlapping lengths were 10 mm as well as 20 mm. The testing series with an overlapping length of 35 mm according to DIN EN ISO 14273 served as reference.

The overlapping lengths were tested with the welding parameters  $h = 1.5$  mm and  $I = 350$  kA. These parameters were chosen, as the transgression to the stable process window is at  $I = 350$  kA, thus, allowing to illustrate the influence. However, an increase of amperage would allow the transgression into the stable process window, also for smaller overlapping lengths. The dependence of the overlapping lengths is shown in Fig. 9.

The reduction of the overlapping length from 35 to 20 mm causes a slight decrease in strength (approximately 11%). This effect is clearer for overlapping lengths of 10 mm (rel.  $\sigma = 0.29$ ); in comparison to the reference series with an overlapping length of 35 mm (rel.  $\sigma = 0.76$ ), the strength values sink by about 52%. The dispersion of the values is also very high. The fracture pattern explains why the welds failed (Fig. 10). The testing series with an overlapping length of 10 mm shows occasional defects in the weld formation. The density of the weld is striking, though, especially in comparison to the weld

with an overlapping length of 20 mm where the density is lower and not developed around the entire weld seam.

The physical process parameters offer an explanation for the decrease in strength. If the overlapping length is too short, the magnetic field which is induced into the testing sample (flyer) can lead to insufficient impact velocities. This can have the effect that the necessary pressure at the collision point for the activation of the weld formation and, thus, the resulting weld is not enough. As a consequence, this leads to a decline of the energy necessary for plastic deformation, which negatively affects the weld properties. As the acceleration distances were the same, the collision angles were also nearly the same for all testing samples, regardless of the overlapping length. However, the question remains whether the geometric impact conditions are met by the samples with short overlapping lengths. The asymmetry in the fracture pattern indicates that, caused by the low impact velocities, the collision angle of the impact, respectively the first collision angle, was too small.

Variations of the angle offer a further interesting effect as regards weld seam pre-treatment or product design. Here, tests were performed to define possible limits of positioning. Figure 11 schematically shows the test setup and the results of the quasi-static tensile shear tests. The parameters of the reference welds were  $h = 1.5$  mm,  $I = 350$  kA and the overlapping length was 35 mm. The current was the same in all

**Fig. 7** Fracture pattern after peel testing according to DIN EN ISO 14270

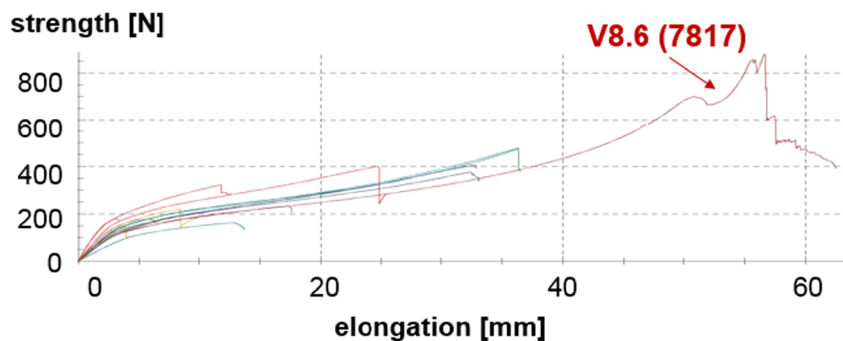
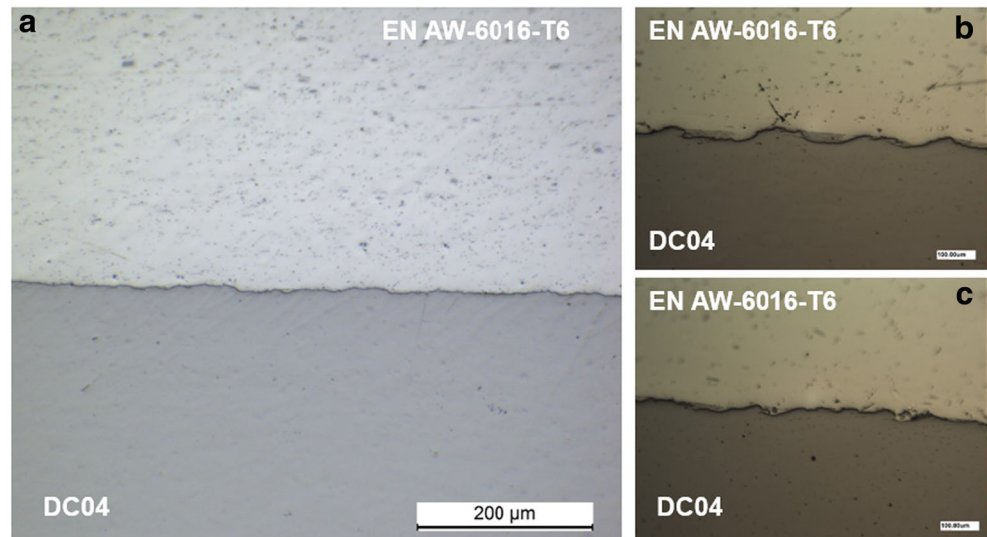


**Fig. 8** Microsections of the material combination EN AW-6016-T6 and DC04



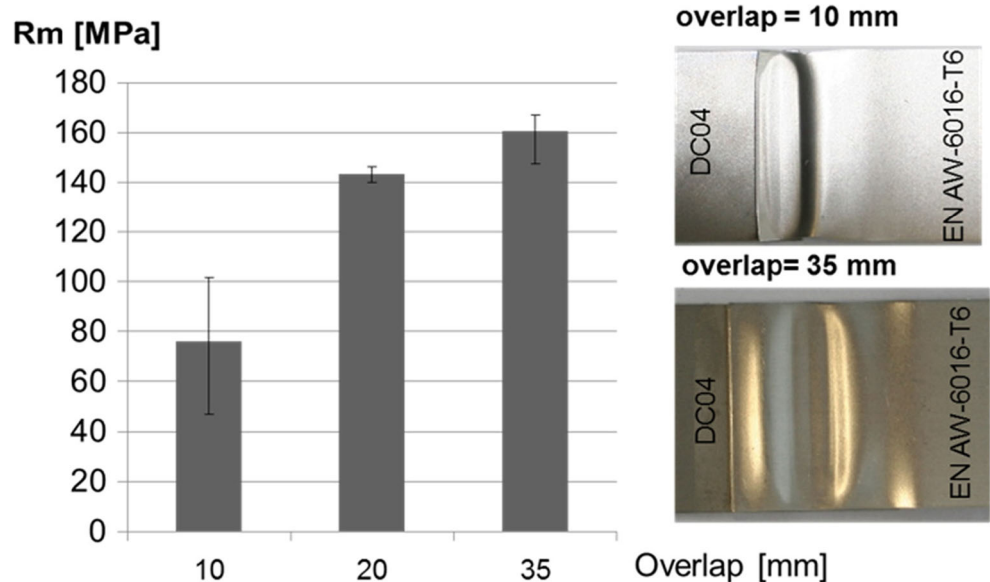
tests; only the acceleration distance changed due to varying positions of the components (depending on the specific variation of the angle).

The results of variations of the angle on the *z*-axis are especially negative. An angle of 5° is enough to reduce the strength of the weld by more than 60%. At an angle of 15°, weld formation could not be realized. Variations of the angle on the *x*-axis offer better results. If the flyer or the target deviates by 15°, about 22% of the strength is lost. If the deviation is 15°, the strength decreases by about 40% in comparison to the reference weld.

The examination of all the results on the influence of production fluctuations and tolerances allows the following conclusions: As soon as the critical energy level which consists mainly of kinetic energy for plastic deformation is bridged,

different acceleration distances can be overcome without changing the strength values significantly. When setting the process parameters, the direction-dependent stress characteristics need to be taken into account, i.e., the type of stress has to be considered. For example, short acceleration distances with small collision angles achieve a higher density of the weld seam. Here, the basic prerequisites are high impact velocities and the accompanying high pressure in the collision angle. In this case, the unrolling process occurs under small collision angles. As a result, the jet can prepare the surface for the weld formation and assists the plastic deformation (Fig. 12). However, if the acceleration distance is changed, e.g., deviation of the angle, especially on the *z*-axis, the aforementioned physical process parameters cannot begin the weld formation and can impair the strength values of the weld seam.

**Fig. 9** Influence of the different overlapping lengths





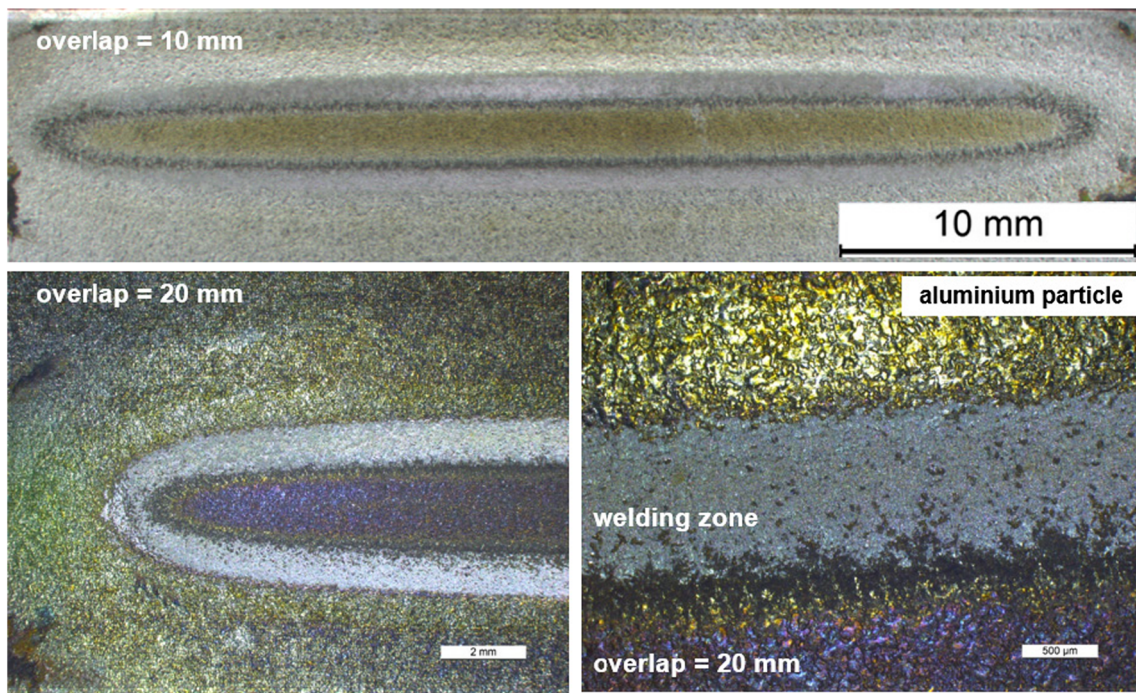


Fig. 10 Fracture pattern analysis of DC04 with an overlapping length of 10 mm as well as 20 mm

### 4.3 Corrosion and thermal shock testing

To determine the aging behavior, a neutral salt spray test according to DIN EN ISO 9227 as well as a thermal shock test according to VDA-233-102 was performed. Here too, the material combination of EN AW-6016-T6 and DC04 was tested. The welding parameters were set to the optimal use. The acceleration distance was 1.25 mm and the maximum amperage was 370 kA. First, the quality of the weld seam was

determined via tensile shear testing according to DIN EN ISO 14273. Laser ablation was applied for DC04 as sample pre-treatment. After welding, the samples were coated with a cathodic dip painting (KTL) layer (Fig. 13).

Concluding from the results, mixed-material combinations are well suited for magnetic pulse welding and there is sufficient aging resistance. No decrease in strength could be detected, especially after the test according to DIN EN ISO 9227; even after a stress period of 1000 h,

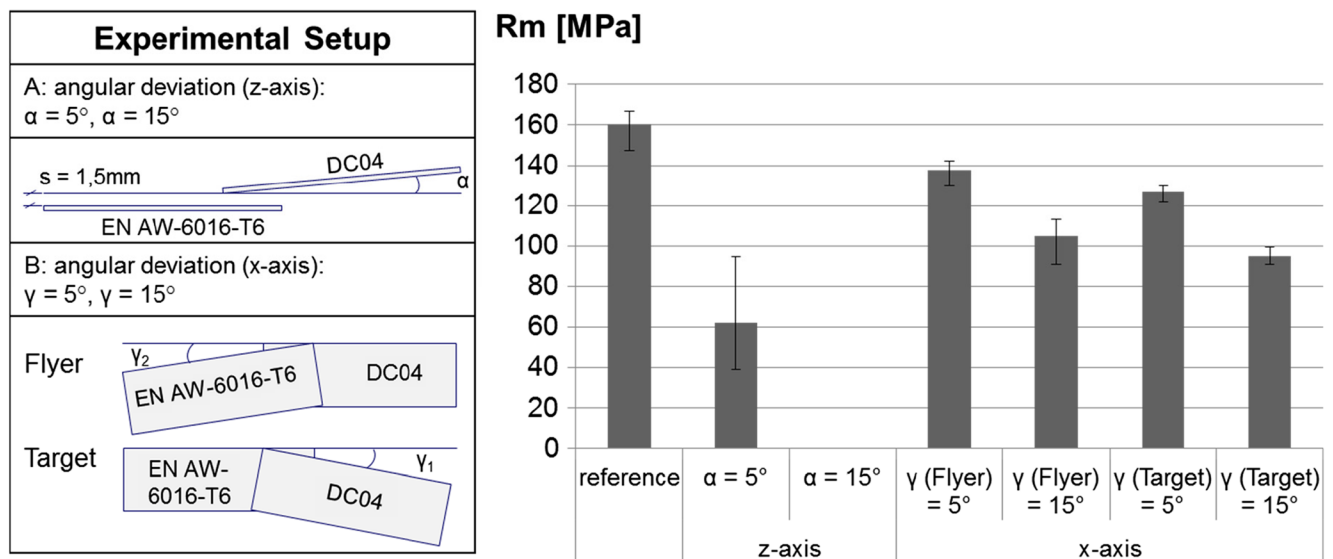


Fig. 11 Influence of the deviation of the angle

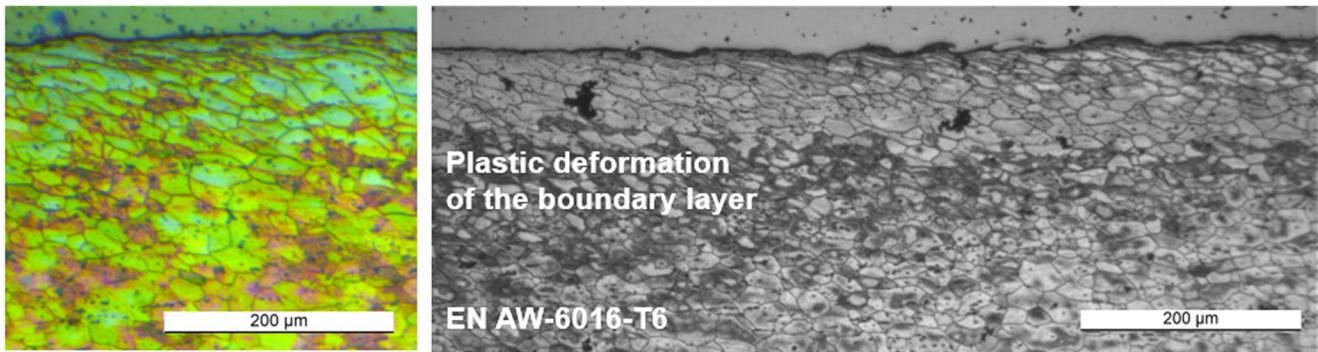


Fig. 12 Plastic deformation during weld formation

the strength values were on a high level and reproducibility was high.

However, the fracture patterns after the salt spray test offer interesting insights. Figure 14 shows a testing series which was exposed for 480 h. The weld seam stayed untouched by the corrosion, only the pressurized zone shows corrosion. This also shows that the overlapping area (outside of the weld seam) has some flaws. In these cases, there was no KTL coating. A reason could be that the wetting was not complete. Possible air pockets left over after the coating process prevented the complete coating. Thus, no galvanic isolation between the corrosion partners occurred during the salt spray test and the thermal shock test. Figure 14 also shows that the KTL coating had burst off in some places. A comparison to the samples which were exposed for 1000 h clearly shows a connection to the contact corrosion. As soon as there was an electrolyte, the aluminum as the more ignoble metal lost much material. However, the weld seam was not affected by this and salt spray testing showed no decrease in strength.

The VDA-233-102 test offered slightly worse results. The coating was the problem here, too; it seems that air pockets caused the flaws in the coating. This could

explain the high dispersion of the strength values. However, in sum, aging resistance can be ensured even if the protection against corrosion is not optimal, especially as there was no passive protection from corrosion for the steel alloy.

#### 4.4 Weldability of high-strength and ultra-high-strength steels

The main tests which were performed with the previously mentioned material combination assisted in gaining information about the robustness of the welding process. One important finding is that it is possible to transfer the method of magnetic pulse welding to other material combinations. Here, high-strength and ultra-high-strength steels present an interesting target as the conventionally used welding methods (e.g., rivets) which are the state of the art reach their limits when welding high-strength and ultra-high-strength materials.

Different steel alloys were examined regarding their suitability for magnetic pulse welding. The strengths of the steels were between 420 and 1500 MPa. Figures 15 and 16 show an overview of the achieved strengths of the mixed-material welds. The acceleration distance was set

Fig. 13 Results of the corrosion and the thermal shock tests

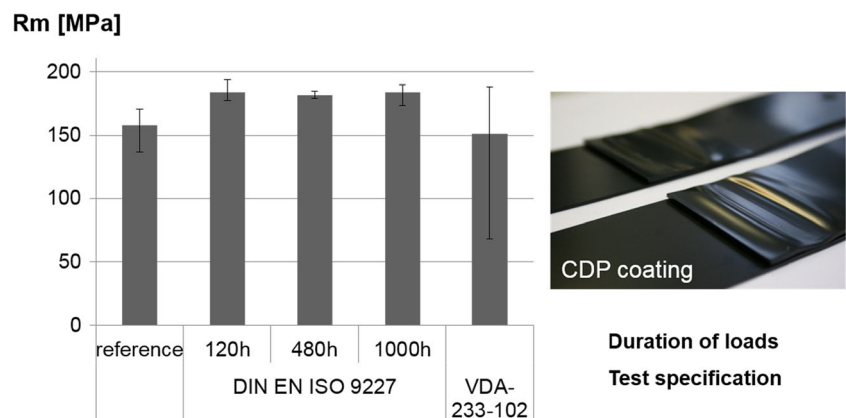
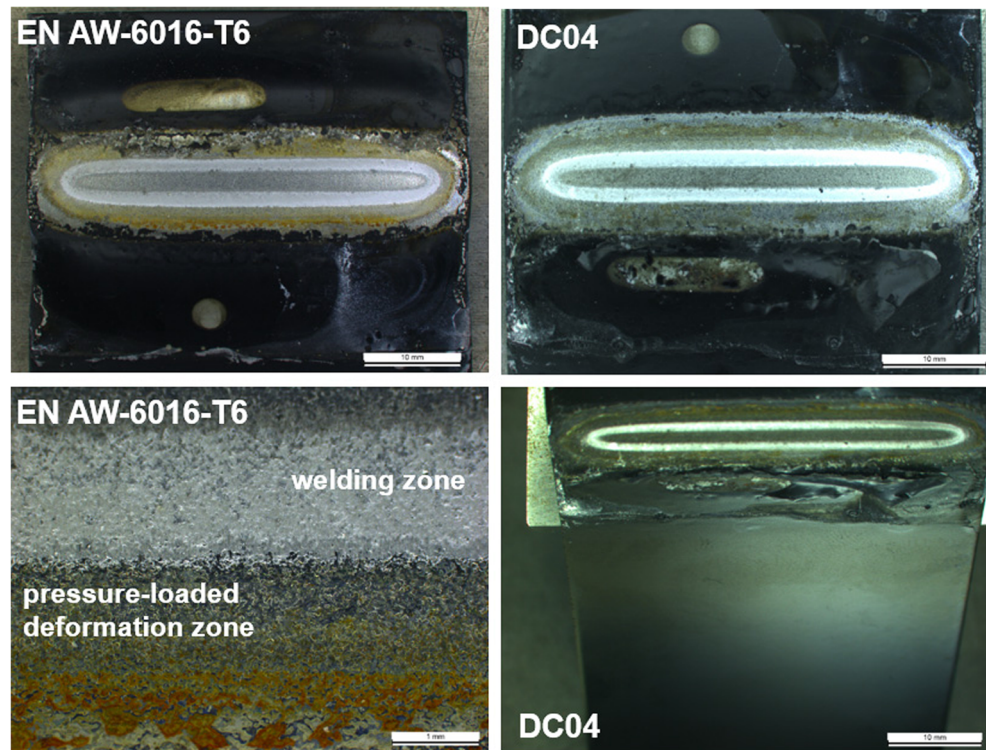


**Fig. 14** Fracture pattern analysis after salt spray testing, period of exposure 480 h



to 1.5 mm for all testing series. Maximum electric currents were discharge frequencies of 19.7 kHz to 350 kA.

When looking at the results, it is striking that the relative strength of the weld decreases with increasing strength of the steel alloy. In those locations where the material combination EN AW-5754-22 with HX420LAD + Z100 failed in the pressurized deformation zone of the aluminum (rel.  $\sigma = 0.96$ ), testing samples with high-strength steel alloys showed lower strengths of the weld. The coating of all steel alloys was removed

by polishing (e.g., AS 150). However, the alloy DP780 + GI was an exception. The combination of drilling manganese steel with EN AW-5754-H22 achieved an especially high relative strength of 0.37.

These strength values show that even welding along the lower process window can achieve high relative strengths. The welds are exemplarily shown with the according microsection in Fig. 17. All testing series showed no indications for structural transformations. In addition, the interface of the weld seam was developed differently

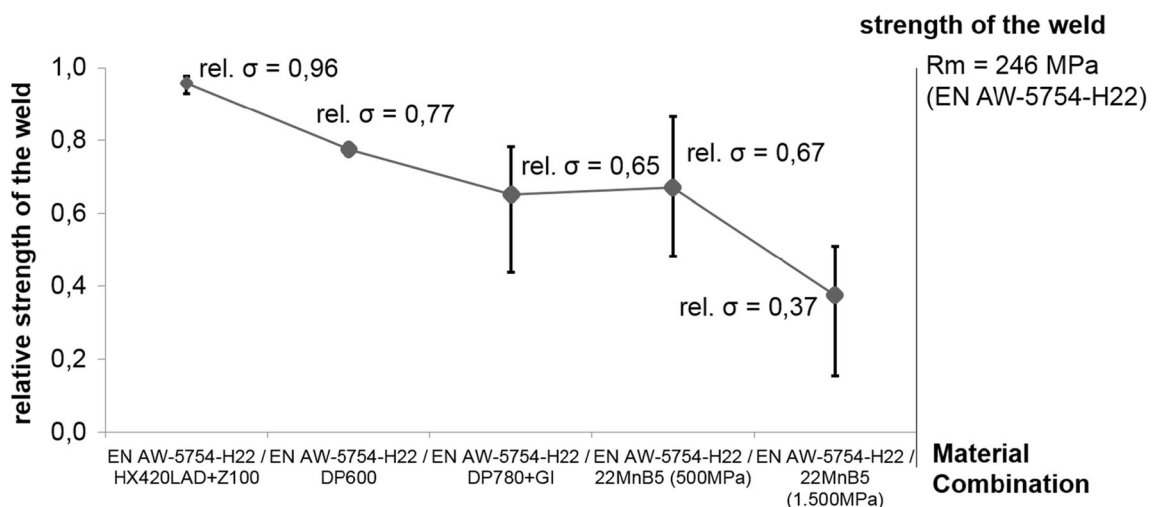
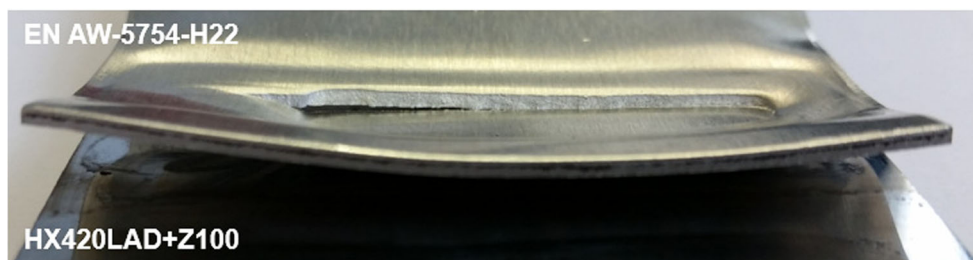


**Fig. 15** Relative strengths of the material combination EN AW-5754-H22 and high-strength and ultra-high-strength steels

**Fig. 16** Fracture pattern analysis of the material combination EN AW-5754-H22 and HX420LAD + Z100; failure in the base material of the aluminum alloy



(e.g., wave formation of the weld of EN AW-5754-H22 and DP600).

All in all, the results show that the stronger the steel alloy of the welding partner, the higher the necessary current needs to be set. Thus, higher collision point velocities can be achieved and the energy input for the plastic deformation can exceed the critical weld seam boundary. As a result, we can assume that if  $I = 370$  kA, higher weld seam strengths can be achieved

close to the weaker base material (EN AW-5754-H22). Furthermore, the yield strength ratio of the flyer plays an important role, which means that other collision point velocities and collision angles can be achieved for the alloy EN AW-5754-H22 with  $R_m/R_{p0.2}$  of 1.30 in comparison to EN AW-6016-T6 with  $R_m/R_{p0.2}$  of 1.97. These two parameters, on the other hand, contribute much to the plastic deformation and, as a consequence, to the weld formation.

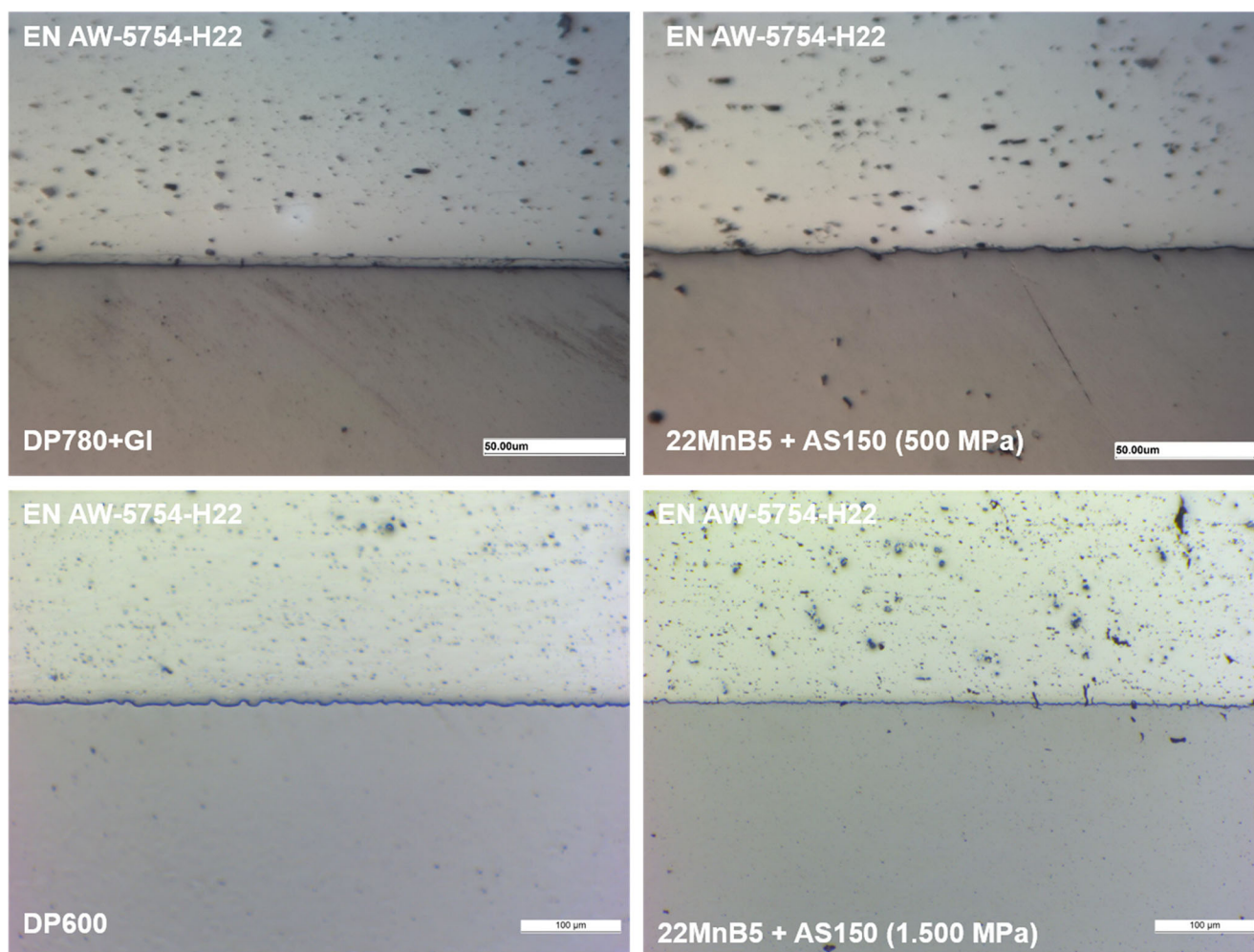


**Fig. 17** Microsections of the aluminum alloy EN AW-5754-H22 and high-strength and ultra-high-strength steels alloys

## 5 Conclusions and outlook

The research aim was to describe the weld formation characteristics of magnetic pulse welding. Knowledge, so far, was based on the description of phenomenological effects (e.g., wave formation). Furthermore, scientific publication and current essays describe the welding of rotationally symmetric components. As regards the material combination, mostly soft alloys were tested. However, it is especially the physical, technological–mechanical properties of impact welding which allow to weld material combinations which are not weldable with other methods. The welding of the material combinations of aluminum and steel alloys is much required and the demand for cold joining processes is increasing constantly, especially for metal sheets.

The results of this study clearly show the high reproducibility of magnetic pulse welding. Even high-strength alloys could be welded with nearly no dispersion of the strength values and strengths close to those of the weaker base material could be achieved (e.g., EN AW-5754-H22 and HX420LAD + Z100 with rel.  $\sigma = 0.96$ ). However, there are still disturbance variables which influence the welding results. One of these variables is the topography of the surface; this can have both a negative effect (e.g., no weld formation) as well as a positive one, an aspect which can be used to shift the process window.

The set amperage is the decisive process parameter for process robustness which determines whether there is a transgression into the stable process window or not. As soon as the lower weld seam boundary is passed, tolerances in forms of deviances in the gap can be overcome. However, this characteristic has to be taken into account when designing the layout of the weld as it is the influence of the acceleration distance and, thus, that of the collision angle which can easily be underestimated. The results show that for shear stress the acceleration distance can be chosen freely as the amplitude of the maximum impulse is the decisive factor. However, if the component is put under peel stress, we can only suggest keeping the acceleration distance as short as possible, however, not smaller than the wall thickness of the flyer.

Two methods were used to test the aging resistance. Both the salt spray test according to DIN EN ISO 9227 as well as the cyclical corrosion test according to VDA 233-102 showed excellent results. Although the KTL coating (cathodic dip painting) was not sufficient in the overlapping area, the weld seam suffered no corrosion. In nearly all cases, the determined strength values showed a high reproducibility. Only contact corrosion occurred due to the insufficient coating of the outer area. In the future, measures to protect the material from corrosion have to be improved. This specifically also refers to passive measures for protection from corrosion which also need to be examined explicitly regarding their influence on the weld formation.

All in all, magnetic pulse welding offers new possibilities for the welding of aluminum–steel welds without the formation of intermetallic phases. As this cold welding method welds so quickly, under 20  $\mu\text{s}$ , it is an excellent method for serial applications and there are most likely still many more possible applications for this method in the future—it definitely has the potential.

**Acknowledgements** The Department for Cutting and Joining Manufacturing Processes would like to thank the accompanying committee for their excellent support. The research project (AiF-Nr. 18290 N/P1029) of the FOSTA Stahlanwendungen e.V. was funded through the program for the promotion of the “Industrial Community Research (IGF)” by the Federal Ministry of Economic Affairs and Energy through the AIF. This assistance is gratefully acknowledged.

## References

1. Trykov YP, Adamenko NA, Sedov EV, Kazurov AV (2003) Titelrussisch. Improving the operational properties of metal–polymer composite materials and goods produced by an explosive treatment. *Masinstroitel* 12:38–40
2. Trykov YU, Gurechov LM, Gurulev DN (2001) Diffusion processes in heating a Ti–Al composite produced by explosion welding. Diffusionsprozesse bei der Erwärmung eines sprenggeschweißten Ti-al-Verbundwerkstoffs. *Weld Int* 15(5):399–401. <https://doi.org/10.1080/09507110109549377>
3. Trykov YP, Gurevich LM, Belousov VP (2003) Special features of production of composite membranes with a tantalum coating from blanks produced by explosive welding. *Weld Int* 17(1):67–69. <https://doi.org/10.1533/wint.2003.3083>
4. Trykov YP, Dolgii YG, Pronichev DV (2001) Special features of manufacture of ring-shaped transition pieces from explosion-welded, steel–aluminium blanks. Besondere Merkmale der Fertigung ringförmiger Zwischenstücke aus sprenggeschweißten Stahl-Aluminium-Rohlingen. *Weld Int* 15(1):41–44. <https://doi.org/10.1080/09507110109549314>
5. Aizawa T, Kashani M, Okagawa K (2007) Application of magnetic pulse welding for aluminum alloys and SPCC steel sheet joints
6. Bertelsbeck S, Geyer M, Böhm S (2012) Magnetic impulse welding of flexible tubes. Denver, Colorado
7. Kahraman N, Güleç B, Findik F (2005) Joining of titanium/stainless steel by explosive welding and effect on interface. *J Mater Process Technol* 169(2):127–133. <https://doi.org/10.1016/j.jmatprotec.2005.06.045>
8. Lee K-J, Kumai S, Arai T, Aizawa T (2007) Interfacial microstructure and strength of steel/aluminum alloy lap joint fabricated by magnetic pressure seam welding. *Mater Sci Eng A* 471(1–2):95–101. <https://doi.org/10.1016/j.msea.2007.04.033>
9. Schaefer R, Pasquale P, Elsen A (2010) Material hybrid joining of sheet metals by electromagnetic pulse technology. pp 61–68
10. Marya M, Rathod M, Marya S, Kutsuna M, Priem D (2007) Steel-to-aluminum joining by control of interface microstructures—laser-roll bonding and magnetic pulse welding, pp 4013–4018
11. Shim J-Y, Kim I-S, Kang M-J, Kim I-J, Lee K-J, Kang B-Y (2011) Joining of aluminum to steel pipe by magnetic pulse welding. Verbinden von Aluminium mit Stahlrohr durch Magnetimpulsschweißen/aluminum alloys: their physical and mechanical properties, ICAA, International Conference on Aluminium Alloys, 12. *Mater Trans* 52(5):999–1002. <https://doi.org/10.2320/matertrans.L-MZ201131>

12. Stern A, Aizenshtein M (2002) Bonding zone formation in magnetic pulse welds. *Sci Technol Weld Join* 7(5):339–342. <https://doi.org/10.1179/136217102225002673>
13. Mehnert S (2001) Auslegung magnetumgeformter Verbindungen durch Simulation. Deutsche Dissertation, Fraunhofer- Institut f. Produktionsanl. u. Konstruktionstechn. (IPK)
14. Beerwald C (2005) Grundlagen der Prozessauslegung und -gestaltung bei der elektromagnetischen Umformung. Monographie. Institut für Umformtechnik und Leichtbau, Universität Dortmund de, Dortmund
15. Henselek A, Beerwald M, Beerwald C (2004) Design and adaptation of EMF equipment—from direct acting multi-turn coils to separable tool coils for electromagnetic tube compression, pp 275–284
16. Aizawa T, Kashani M, Okagawa K (2012) Welding and forming of sheet metals by using magnetic pulse welding (MPW) technique
17. Desai SV, Kumai S, Satyamurthy P, Chakravarty JK, Chakravarty DP (2010) Scaling relationships for input energy in electromagnetic welding of similar and dissimilar metals, pp 563–570
18. Kore SD, Date PP, Kulkarni SV, Kumar S, Rani D, Kulkarni MR, Desai SV, Rajawat RK, Nagesh KV, Chakravarty DP (2012) Application of electromagnetic impact technique for welding copper-to-stainless steel sheets
19. Shim J-Y, Kim I-S, Lee K-J, Kang B-Y (2011) Experimental and numerical analysis on aluminum/steel pipe using magnetic pulse welding. *Met Mater Int* 17(6):957–961. <https://doi.org/10.1007/s12540-011-6014-8>
20. Crossland B (1982) Explosive welding of metals and its application. Clarendon Press, Oxford
21. Geyer M, Rebensdorf A, Böhm S (2014) Influence of the boundary layer of magnetic pulse welds between aluminum and steel, 6th International Conference on High Speed Forming
22. Geyer M (2016) Magnetpulsschweißen von Aluminium und Stahl – Einflüsse der Topografie auf Verbindungs-ausbildung und Festigkeit, Dissertation, Kassel
23. Rebensdorf A, Böhm S (2016) Increase of the reproducibility of joints welded with magnetic pulse technology using graded surface topographies. 7th International Conference on High Speed Forming